# MEASUREMENT OF DISPLACEMENT FIELDS WITH SUB-PIXEL ACCURACY BY COMBINING CROSS-CORRELATION AND OPTICAL FLOW

**A. M. R. Sousa[1], J. Xavier[1], M. Vaz[2], J. J. L. Morais[1], V. M. J. Filipe[1]**

[1] CITAB, Engineering Department, University of Trás-os-Montes and Alto Douro
[2] Mechanical Engineering Department, Faculty of Engineering of University of Porto



***ABSTRACT***

*This paper presents a method to measure the displacements fields on the surface of a planar object with sub-pixel resolution, by combining image correlation and a differential technique. First, a coarse approximation of the pixel level displacement is obtained by cross correlation (CC). Two consecutive images, taken before and after the application of a given deformation, are recursively split in sub-images, and the CC coefficient is used as the similarity measure. Secondly, a fine approximation is performed in order to assess the sub-pixel displacements by means of an optical flow method based on a differential technique. This differentiation is achieved in a window of pixels that will typically define the displacement spatial resolution of the method. In order to validate the effectiveness and robustness of the proposed method, numerical tests, consisting of a rigid-body translation test and a rotation test, were carried out on computer generated images.*

## 1 - INTRODUCTION

The measurement of the displacement field from a sequence of images of an object when this is moved or deformed by an external action, is a relevant information in many fields of digital image processing, such as motion estimation (Aggarwal and Nandhakumar 1988), image measurement (West and Clarke 1990) or image registration (Tian and Huhns 1986). In the last decades, many techniques used in these fields have assumed greater importance in the framework of experimental solid mechanics (Sutton et al. 2009). The major advantages of using optical methods, over more conventional point-wise measuring techniques, such as strain gauges, are the assessment of full-field data and their non-evasive nature. Besides, among other proposed full-field optical methods for displacement or strain measurement, such as grid methods (Xavier et al. 2007), interferometric moiré or speckle methods (Cloud 1995), image correlation requires relatively simple photo-mechanical set-up and preparation of the surface of specimens. In this technique, the displacement field is measured by following the evolution of a textured pattern (usually a random speckle pattern) and is insensitive to vibration (Yaofeng et al. 2005), enabling the accurate extraction of surface displacement.

In digital image correlation (DIC) algorithms, pixel level displacements between pairs of images are obtained searching the minimum or maximum likelihood from the similarity or dissimilarity of images regions. Either, the

sum of absolute differences (SAD), the sum of squared differences (SSD) or the cross correlation (CC) are usually used to evaluate the matching between regions (Hill et al. 2006; Chu et al. 1985). Greater resolution can be achieved when sub-pixel information is calculated increasing the accuracy of the displacement field characterisation. There are a wide variety of algorithms performing this calculation (Aggarwal and Nandhakumar 1988), although they can be classified into four categories (Tian and Huhns 1986): image interpolation, similarity interpolation, gradient-based and phase-correlation method. DIC was first proposed by Sutton and co-workers (Chu et al. 1985). They used coarse-fine search to find the accurate displacements at pixel level, and the sub-pixel accuracy was achieved by combining the intensity pattern of an image with bilinear, polynomial or bi-cubic spline.

In this paper, a coarse-fine approach is proposed where a coarse pixel level displacement approximation is obtained by cross correlation. At this stage, two consecutive images are recursively split in sub-images, and the CC coefficient is used as the similarity measure. In the second stage, a finer approximation is performed to obtain sub-pixel displacement calculated using an optical flow method (Horn and Schunk 1981; Lucas and Kanade 1981; Nagel 1983; Uras et al. 1988; Anandan 1987; Singh 1990; Heeger 1987; Waxman and Wohn 1985; Fleet and Jepson 1990) based on a differential technique.

The proposed method is explained in full detail in section 2. The effectiveness of the method is validated using numerical tests (rigid-body translation and rotation test) and the results are presented in section 3. Some conclusions and final remarks are addressed in section 4.

## 2 - PROPOSED METHOD

The proposed method follows a 2 steps coarse-fine approach: pixel level estimation (coarse) and sub-pixel level estimation (fine) of displacement fields. In the first step, the normalized cross-correlation is recursively applied over the sub-images obtained over the original images pair, using a quad-tree splitting process. On the second step an optical flow method based on a differential technique is used. One of the limitations of optical flow is related with image intensity which must be nearly linear across a given period of time (Barron et al. 1994). The direct application of optical flow to calculate the displacements field on the surface of a specimen that undergoes a large deformation in a short period of time would introduce considerable errors in the resulting displacement fields.

Therefore, in the proposed method a first step is introduced to calculate the pixel level displacement of each sub-image. This procedure reduces to a minimum the pixel level displacement of each pixel inside a sub-image (after being shifted) fulfilling this way the optical flow constraint. This enables optical flow technique to perform accurate measurement of sub-pixel displacement.

### 2.1 - Pixel level estimation

The pixel level displacement estimation is performed over a pair of images obtained before (reference) and after surface deformation (deformed). Using a quad-tree process each image is divided into a set of sub-images and a normalized cross correlation is applied to obtain the displacement of each sub-image centre point.

#### 2.1.1 *Cross correlation*

To perform this task each sub-image in the reference image is used to map another sub-image on the deformed image. The matching of a sub-image is found by maximizing the normalized cross correlation coefficient between intensity patterns of two sub-images.

$$c(u,v) = \sum_{x,y} f(x,y)t(x-u,y-v) \qquad (1)$$

Eq. (1) is a measure of the similarity between the image $f$ and the feature $t$. Among others disadvantages in using $c(u,v)$ for template matching, it can be noticed that the range of $c(u,v)$ is dependent on the size of the feature and is not invariant to changes in image amplitude, such as those

caused by changing lighting conditions across the image sequence.

The correlation coefficient overcomes these difficulties by normalizing the image and feature vectors to unit length, yielding a cosine-like correlation coefficient

$$\gamma(u,v) = \frac{\sum_{x,y}\left[f(x,y)-\bar{f}_{u,v}\right]\left[t(x-u,y-v)-\bar{t}\right]}{\left\{\sum_{x,y}\left[f(x,y)-\bar{f}_{u,v}\right]^2 \sum_{x,y}\left[t(x-u,y-v)-\bar{t}\right]^2\right\}^{0.5}} \quad (2)$$

where $\bar{t}$ is the mean of the feature and $\bar{f}_{u,v}$ is the mean of $f(x,y)$ in the region under the feature. $\gamma(u,v)$ is referred as the normalized cross-correlation (Lewis 1995; Haralick and Shapiro 1992).

### 2.1.2 *Quad-tree image splitting*

The image splitting is similar to a quad-tree division process and is used to enable coarse pixel level displacements estimation between reference and deformed image, following a global to local approach. First a global displacement between full sized images is calculated using the similarity measurement. Next, both images (reference and deformed) are submitted to the splitting process using a quad-tree technique which consists in dividing each one recursively into four (4) sub-images (Fig. 1) and repeating for each pair the normalized cross-correlation calculation.

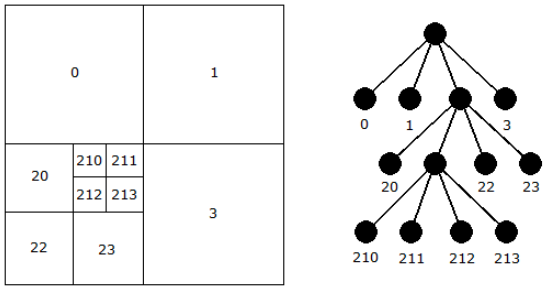


**Fig. 1** – Quad-tree image splitting process.

At any level $n$ of the splitting process (Fig. 2), the obtained displacement is assumed constant along the entire sub-image; notice that sub-image at level $n = 0$ represents the entire image. After the splitting process terminates, a coarse map of pixel level displacements between reference and deformed image is obtained from their sub-images.

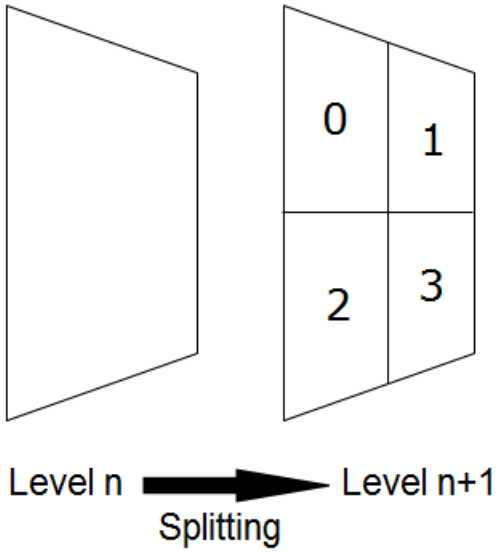


**Fig. 2** – Splitting process at level n resulting in 4 sub-images.

The maximum number of splitting levels can be defined by:

$$n_{max} = \log_2 \frac{min_{l,c}}{2} \quad (3)$$

where,

$$min_{l,c} = \begin{Bmatrix} lines, & lines \le columns \\ columns, & columns < lines \end{Bmatrix}, (lines, columns)\ size\ of\ image \quad (4)$$

From Eq. (3) the smallest sub-image size is given by:

$$s = \frac{min_{l,c}}{2^n},\ s\ must\ be\ an\ integer\ value \quad (5)$$

The splitting process of a certain sub-image at level $n$ stops when at least one of three conditions is satisfied: 1) the maximum number of splitting levels defined in Eq. (3) is reached; 2) the displacement calculated from level $n$ to level $n+1$ doesn't follow a smooth behaviour; 3) or is the same. The expressions defining these conditions are expressed as follows:

1) $n = n_{max}$ (6)

2) $abs(d_{n+1} - d_n) > 1$ (7)

3) $d_{n+1} = d_n$ (8)

Where *m* is the current splitting level of the method and $d_n$ and $d_{n+1}$ represents respectively the displacement of image at level n and n+1.

## 2.2 - Sub-pixel level estimation

After finding a coarse pixel level displacement between the two images, sub-pixel estimation is applied to obtain greater resolution. Each reference sub-image (resulting from the quad-tree decomposition) is shifted by their amount of pixel level displacement over the correspondent deformed sub-image. Next, the displacement estimation of each pixel belonging to the sub-image is computed using an optical flow technique (OF). The goal of OF is to compute an approximation to the 2D motion field – a projection of the 3D velocities of surface points onto the imaging surface – from spatiotemporal patterns of image intensity. The main stages of processing consist of: 1) prefiltering or smoothing with low-pass / band-pass filters (to extract signal structure of interest and enhance SNR (signal-to-noise ratio); 2) the extraction of basic measurements such as spatiotemporal derivatives (to measure normal components of velocity); 3) the integration of the previously extracted measurements to produce a smooth 2D flow field. The method proposed in this paper implements a first-order technique, more specifically, the local differential technique from Lucas & Kanade (Lucas and Kanade 1981), which has been proved to be an efficient and reliable technique (Barron et al. 1994; Pan et al. 2006).

### 2.2.1 *Spatio-temporal derivatives*

Differential techniques compute velocity from spatiotemporal derivatives of image intensity (I) or filtered versions of the image using low-pass or band-pass filters. In the present case a Gaussian filter is used. The main requirement for differential techniques is that $I(x,t)$ must be differentiable. The technique proposed by Lucas & Kanade implements weighted least-squares (LS) fit of local first-order constraints to a constant model for $v$ in each small spatial neighbourhood Ω of position $x = (x,y)$, by minimizing:

$$\sum_{x\in\Omega} W^2(x)[\nabla I(x,t)\cdot v + I_t(x,t)]^2, \quad (9)$$

$W(x)$ is a window function that gives more influence to constraints at the centre of the neighbourhood than at the periphery. Depending on the speckle size, this function could be adjusted in order to control the spatial resolution (i.e., the windows size). $\nabla I(x,t)$ is the spatial intensity gradient, $\vec{v} \rightarrow (Vx, Vy)$ represents the two components image velocity and $I_t(x,t)$ is the partial time derivative of image intensity at position *x* in instant *t*. The displacement field resulting from differential technique has sub-pixel resolution usually with values less than 1 pixel.

The global displacement of each pixel is then obtained by adding its coarse pixel level displacement (cross-correlation) with the respective finer sub-pixel level displacement (differential technique).

# 3 - PERFORMANCE ASSESSMENT OF THE PROPOSED METHOD: RESULTS AND DISCUSSION

## 3.1 - Validation procedure

In order to assess the performance, i.e. the sensitivity and the accuracy of optical methods both numerical (Lecompte et al. 2006; Bing et al. 2006) and experimental (Wang and Cuitino 2002; Haddadi and Belhabib 2008) tests can be carried out. In these tests, the underlying idea is to compare a known displacement field, which is applied to move or deform a given textured pattern reference, with the one calculated by the proposed method (Fig. 3).

For the purpose of validation, it can be advantageous to perform numerical analyses by processing computer-generated speckle-pattern images (Orteu et al. 2006; Bornert 2007). In this approach the errors associated to the proposed method can be uncoupled from the experimental ones (e.g., light intensity variation or error in imposing

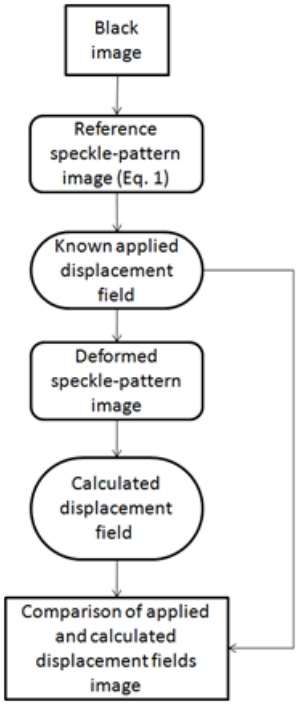


**Fig. 3** – Flowchart representation of the computer-generated speckle-pattern images.

a reference displacement). Moreover, more complex (e.g., heterogeneous) deformation fields can be analysed, since experimentally only simple controlled tests such as static (motionless) or rigid-body tests (i.e., in-plane or out-of-plane translations and rotations) can be carried out. Numerically, several tests can be performed on images generated before and after the application of a prescribed displacement or strain field. Such tests can consist of: rigid-body translation and rotation tests, homogeneous tests (i.e., associated to uniform strain fields) and heterogeneous tests (i.e., associated to non-uniform strain fields) (Lecompte et al. 2006; Bing et al. 2006; Orteu et al. 2006; Bornert 2007).

### 3.2 - Generation of synthetic speckle-pattern images

When using numerical tests, one major difficulty is the generation and deformation of a realistic synthetic speckle-pattern image, i.e., with a histogram and spectral properties similar to the ones of real speckle images which can be obtained, for instance, by spray painting or toner powder deposition (Orteu et al. 2006). Several authors (Bing et al. 2006; Wattrisse et al. 2001) have proposed analytical expressions for generating this type of synthetic images. The advantage is that an analytical displacement field can be directly used in order to deform a given reference speckle-pattern image. Thus, images corresponding to undeformed ($I_i$) and deformed ($I_f$) configurations can be generated according to the following expressions:

$$I_i(x,y) = \sum_{k=0}^{N_s} I_k exp\left\{-\frac{(x-x_k)^2+(y-y_k)^2}{R^2}\right\} \tag{10}$$

$$I_f(x,y) = \sum_{i=0}^{N_s} I_i exp\left\{-\frac{\left[x-x_k-U_{ap}^f(x,y)\right]^2+\left[y-y_k-V_{ap}^f(x,y)\right]^2}{R^2}\right\}$$

where $(x,y)$ are the pixel coordinates (corresponding to the sampled unit cells of the CCD sensor), $I^0$ represent a random light intensity value defining the contrast of the speckle image, $R$ controls the granular size of the speckle pattern, $(N_s)$ is the total number of spots defining the textured pattern and $U_{ap}$ and $V_{ap}$ are the applied displacement fields through $x$ and $y$ directions, respectively.

In practice, images with a depth of 8 bit were created as follows. Firstly, a pure black image was generated by initialising a $H \times V$ matrix filled with zeros, where $H$ and $V$ represent, respectively, the length and the width of the image – this could correspond experimentally to cover the region of interest of a sample with black paint, by means of a spray or airbrush for instance. Secondly, the reference speckle-pattern image (undeformed configuration) was generated by iteratively superimposing images with a single randomly distributed gray scale spot characterised by a radius $R$ and having a Gaussian distribution function – in practice, the resulting image could correspond to randomly spread white paint over the black background surface of the sample. The total number of spots $(N_S)$, as well as their central location $(x_k, y_k)$ within the spatial domain of the image was randomly chosen. A sequence of images corresponding to a given undeformed configuration can then be generated, with regard to the reference speckle-pattern image, by applying an inverse displacement field $(U_{app}, V_{app})$ (Eq. 11). Finally, a 5x5

Gaussian filter was applied to the generated images in order to obtain a smooth textured speckle-pattern. An example of a speckle-pattern image, together with its histogram, typically generated from this approach, is shown in Figure 4.

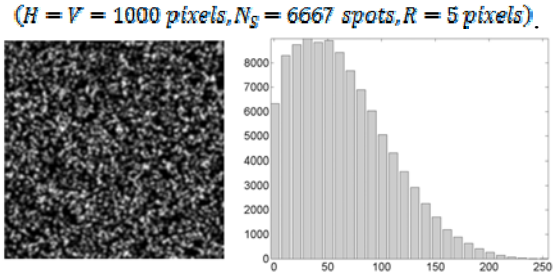


**Fig. 4** – Typical generated speckle-pattern image and its histogram.

## 3.3 - Reconstruction of the kinematic fields

The displacement field determined from the proposed method can be smoothed afterwards by fitting a 2D polynomial function using the least-squares approximation scheme (Xavier et al. 2007):

$$\min_{\{a_\beta\}} \; w \left(u_\beta - \sum_{i,j}^{d} a_{\beta_{ij}} x^i y^j\right)^2 \quad (i+j<d) \qquad (11)$$

where w represents a weighting mask defining the validity of each pixel, $a_{\beta_{ij}}$ $(\beta = x, y)$ are the unknown polynomial coefficients, and d is the degree of the polynomial. In proposed method, a 3th-degree polynomial was found suitable for the least-squares regression scheme. From these smooth displacement fields, the strain fields can be then straightforward reconstructed by analytical or numerical differentiation (Xavier et al. 2007). This approach is suitable since only homogeneous strain fields are to be processed in the numerical tests analysed in the following.

## 3.4 - Numerical tests

In this work, two types of numerical tests were carried out in order to validate the proposed method: (1) an in-plane rigid-body translation test, and (2) a rotation test.

### 3.4.1 *Rigid-body translation test*

The rigid-body translation test consisted in analysing a set of images generated by applying incrementally sub-pixel displacements to a reference image along one direction. Therefore, transformed images were generated with regard to the reference one by cumulatively imposing a translation of 0.1 pixels in the $x$ (column) direction up to 1 pixel. These images were then processed by the proposed method (differentiation window of 9x9 pixels) in order to retrieve the applied uniform displacement fields.

For each calculation (between the reference and each transformed image), determined from the proposed method, the mean displacement value, over the entire field, was evaluated and compared to the applied translation field. This study is summarised in Figure 5a). From these results, a qualitative agreement was found among the calculated and the reference applied displacements. From the residual differences between the calculated and the applied displacements, both mean (systematic error in Figure 5b)) and standard deviation (random error in Figure 5c)) values were determined as a function of the applied sub-pixel displacements.

The mean bias error was obtained with the proposed method reaching its maximum value at an applied displacement of 0.5 pixels of about 3.2x10-2. The standard deviation values are plotted in Figure 5c); as can be seen it remains acceptably low.

### 3.4.2 *Rotation test*

The rotation test consisted in analysing a set of images generated by applying a rotation to a reference image centred in the middle of image. Therefore, transformed images were generated with regard to the reference one by cumulatively imposing an increasingly higher rotation up to 0.6 degrees. These images were then processed by the proposed method (differentiation window of 9x9 pixels) in order to retrieve the displacement fields from the applied rotations.

For each calculation (between the refe-

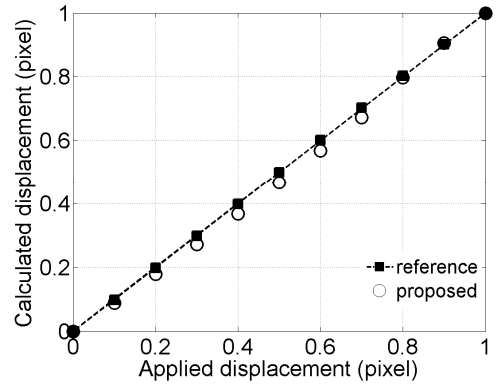


(a)

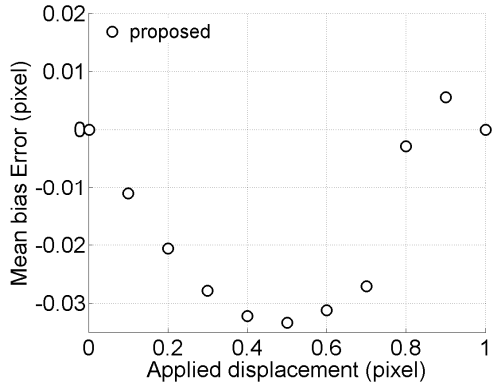


(b)

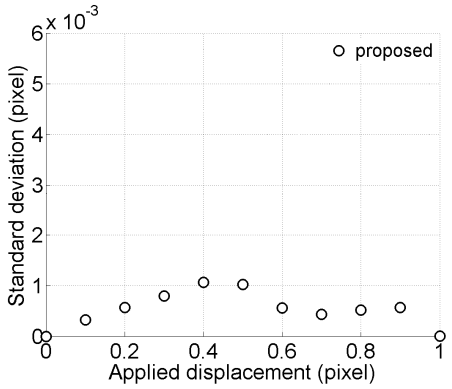


(c)

**Fig. 5** – Calculated displacement (a), mean bias error (b) and standard deviation as a function of the applied displacement (c); unit: pixel.

rence and each transformed image), determined from the proposed method, the displacement values, over the entire field, was evaluated and compared to the applied rotation field. This study is summarised in Figure 6a).

The calculated and the reference applied rotations show similar results. From the residual differences between the calculated and the applied rotations, systematic error

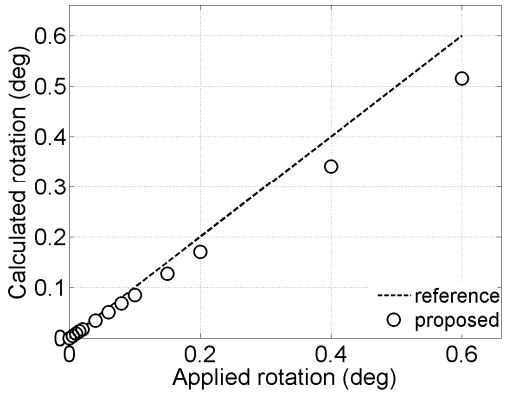


(a)

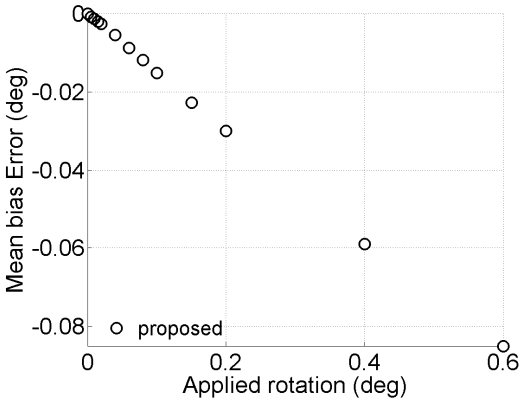


(b)

**Fig. 6** – Calculated rotation (a), mean bias error (b) unit: degrees.

values in Figure 6b) were determined as a function of the applied rotation degrees. The mean bias error was obtained with the proposed method reaching its maximum value at an applied rotation of 0.6 degrees of about -8x10-2.

## 4 - CONCLUSIONS

In this work a method combining cross-correlation and a differential technique was implemented, allowing the measurement of displacement fields with sub-pixel accuracy. It is based on a coarse-fine approach. Coarse approximation is performed using a pixel level estimation (cross-correlation) and the fine estimation by a sub-pixel level estimation approach (differential technique). The computation of the spatial and temporal derivatives is done in a subset that controls the spatial resolution of the technique. Besides, because no local interpolation of the

discrete gray level distribution is required, the proposed method can be eventually applied, in the future, to a wider range of textured patterns.

In order to validate the proposed method two types of numerical tests were carried out: (1) in-plane rigid-body translation test, and (2) rotation test. The method showed accurate and reliable results using numerical tests.

These features along with the quality of results obtained from numerical tests will enable, in future work, the use of proposed method to characterize a wide range of materials and their behaviour (e.g. structural behaviour of fractured objects under load, ex: cortical bone tissue).

## ACKNOWLEDGEMENTS

The authors wish to acknowledge the generous support of the project PTDC/EME-PME/71273/2006, "Comportamento à fractura do tecido ósseo cortical".

## 5 - REFERENCES

Aggarwal, J.K. and Nandhakumar, N. 1988. On the Computation of Motion from Sequences of Images - a Review. Proceedings of the IEEE. 76(8), 917–935.

Anandan, P. (1987). Measuring Visual Motion from Image Sequences. PhD dissertation, COINS TR 87-21, Univ. of Massachusetts, Amherest, MA.

Barron, J.L., Fleet, D.J. and Beauchemin, S.S. (1994). Performance of Optical Flow Techniques. IJCV, 12(1), 43-77.

Bornert, M. (2007). Évaluation métrologique d'algorithmes de corrélation d'images numériques. 18ème Congrès Français de Mécanique, Grenoble, 27-31 août.

Chu, T.C., Ranson, W.F., Sutton, M.A. and Peters, W.H. (1985). Applications of Digital Image Correlation Techniques to Experimental Mechanics. Experimental Mechanics. 25, 232-244.

Cloud, G.L. (1995). Optical methods of engineering analysis. Cambridge University Press, New York.

Fleet, D.J. and Jepson, A.D. (1990). Computation of component image velocity from local phase information. Int. J. Comp. Vision, 5, 77-104.

Haddadi, H. and Belhabib, S. (2008). Use of rigid-body motion for the investigation and estimation of the measurement errors related to digital image correlation technique. Optics and Lasers in Engineering, 46, 185–196.

Haralick, R.M. and Shapiro, L.G. (1992). Computer and Robot Vision. Addison-Wesley II, 316-317.

Heeger, D.J. (1987). Model for the extraction of image flow. J. Opt. Soc. Am., A4, 1455-1471.

Hill, P.R., Chiew, T.K., Bull, D.R. and Canagarajah, C.N. (2006). Interpolation Free Subpixel Accuracy Motion Estimation. IEEE Transactions on Circuits and Systems for Video Technology. 16(12), 1519-1526.

Horn, B.K.P. and Schunk, B.G. (1981). Determining optical flow. Artificial Intelligence, 17, 185-2003.

Lecompte, D., Smits, A., Bossuyt, S., Sol, H., Vantomme, J., Van Hemelrijck, D. and Habraken, A.M. (2006). Quality assessment of speckle patterns for digital image correlation. Optics and Lasers in Engineering, 44(11), 1132-1145.

Lewis, J.P. (1995). Fast Normalized Cross-Correlation, In Vision Interface. Canadian Image Processing and Pattern Recognition Society, 120-123.

Lucas, B. and Kanade, T. (1981). An iterative image registration technique with an application to stereo vision. Proc. DARPA IU Workshop, 121-130.

Nagel, H.H. (1983). Displacement vectors derived from second-order intensity variations in image sequences. CGIP, 21, 85-117.

Orteu, J.-J., Garcia, D., Robert, L. and Bugarin, F. (2006). A spekle-texture image generator. In P. Slangen and C. Cerruti, editors, Speckle06, volume SPIE 6341.

Pan, B., Xie, H.-M., Xu, B.Q. and Dai, F.L. (2006). Performance of sub-pixel registration algorithms in digital image correlation. Measurement Science and Technology, 17(6), 1615-1621.

Singh, A. (1990). An estimation-theoretic framework for image-flow computation. Proc. IEEE ICCV, 168-177.

Sutton, M.A., Orteu, J.-J., Schreier, H. (2009). Image correlation for shape, motion and deformation measurements: Basic concepts, theory and applications, Springer.

Tian, Q. and Huhns, M.N. (1986). Algorithms for Subpixel Registration, Computer Vision, Graphics, and Image Processing. 35, 220–223.

Uras, S., Girosi, F., Verri, A. And Torre, V. (1988). A computational approach to motion perception. Biol. Cybern., 60, 79-97.

Wang, Y. and Cuitino, A.M. (2002). Full-field measurements of heterogeneous deformation patterns on polymeric foams using digital image correlation. International Journal of Solids and Structures, 39, 3777-3796.

Wattrisse, B., Chrysochoos, A., Muracciole, J.-M. and Némoz-Gaillard, M. (2001). Analysis of strain localization during tensile tests by digital image correlation. Experimental Mechanics, 41(1), 29-39.

Waxman, A.M. and Wohn, K. (1985). Contour evolution, neighbourhood deformation and global image flow: Planar surfaces in motion. Int. J. Rob. Res., 4, 95-108.

West, G.A.W. and Clarke, T.A. (1990). A Survey and Examination of Subpixel Measurement Techniques. Proceedings of the SPIE: Close-Range Photogrammetry Meets Machine Vision. 1395, 456–463.

Xavier, J., Avril, S., Pierron, F. and Morais, J. (2007). Novel experimental approach for longitudinal-radial stiffness characterisation of clear wood by a single test. Holzforschung, 61(5), 573–581.

Yaofeng, S., Meng T.Y., Pang, J.H.L. and Fei, S. (2005). Digital Image Correlation and its Applications in Electronics Packaging. Proceedings of the 7th Electronic Packaging Technology Conference (EPTC2005). 1, 129-134